THE JOURNAL OF BIOLOGICAL CHEMISTRY VOL. 285, NO. 37, pp. 28938–28945, September 10, 2010

Impaired *S*-Nitrosylation of the Ryanodine Receptor Caused by Xanthine Oxidase Activity Contributes to Calcium Leak in Heart Failure*[S]

Received for publication, June 18, 2010 Published, JBC Papers in Press, July 19, 2010, DOI 10.1074/jbc.M110.154948

Daniel R. Gonzalez[1], **Adriana V. Treuer**[1], **Jorge Castellanos, Raul A. Dulce, and Joshua M. Hare**[2]

From the Interdisciplinary Stem Cell Institute, Miller School of Medicine, University of Miami, Miami, Florida 33136

***S*-Nitrosylation is a ubiquitous post-translational modification that regulates diverse biologic processes. In skeletal muscle, hypernitrosylation of the ryanodine receptor (RyR) causes sarcoplasmic reticulum (SR) calcium leak, but whether abnormalities of cardiac RyR nitrosylation contribute to dysfunction of cardiac excitation-contraction coupling remains controversial. In this study, we tested the hypothesis that cardiac RyR2 is hyponitrosylated in heart failure, because of nitroso-redox imbalance. We evaluated excitation-contraction coupling and nitroso-redox balance in spontaneously hypertensive heart failure rats with dilated cardiomyopathy and age-matched Wistar-Kyoto rats. Spontaneously hypertensive heart failure myocytes were characterized by depressed contractility, increased diastolic Ca^{2+} leak, hyponitrosylation of RyR2, and enhanced xanthine oxidase derived superoxide. Global *S*-nitrosylation was decreased in failing hearts compared with nonfailing. Xanthine oxidase inhibition restored global and RyR2 nitrosylation and reversed the diastolic SR Ca^{2+} leak, improving Ca^{2+} handling and contractility. Together these findings demonstrate that nitroso-redox imbalance causes RyR2 oxidation, hyponitrosylation, and SR Ca^{2+} leak, a hallmark of cardiac dysfunction. The reversal of this phenotype by inhibition of xanthine oxidase has important pathophysiologic and therapeutic implications.**

Heart failure (HF)[3] is a complex, multi-faceted disorder characterized by depressed contractility of cardiac myocytes and a diverse array of abnormalities in excitation-contraction coupling. It is increasingly appreciated that SR calcium leak through the RyR2 is a central lesion leading to diminished myocyte contraction and electrical instability, which enhances the risk of cardiac arrhythmias (1). With regard to RyR biology, recent reports implicate elevated nitrosylation of RyR1 with SR Ca^{2+} leak and skeletal muscle dysfunction (2–4). Paradoxically, we have shown that in cardiac myocytes of neuronal nitric-oxide synthase (NOS1)-deficient mice, decreased *S*-nitrosylation causes RyR2 leak, decreased contractile reserve, and occurrence of delayed after-depolarizations (5).

One possible explanation for this paradox relates to nitroso-redox imbalance, a condition in which excess formation of reactive oxygen species (ROS) can modify the same thiols that are targets of *S*-nitrosylation, leading to irreversible protein activation (6). Because increased oxidative stress is common in myocardial dysfunction (7), we tested the idea that in the case of RyR2, the channel is hyponitrosylated but similarly subject to SR calcium leak because of increased oxidative modification. The RyR2 is especially sensitive to redox modifications because of the presence of many hyperreactive cysteines (8), which can be *S*-nitrosylated (9), glutathionylated (10, 11), or further oxidized to disulfide bonds.

The purpose of this study was to assess RyR2 nitrosylation and function in a relevant HF model, the SHHF rat. Our results reveal that the channel is hyponitrosylated because of increased oxidative stress, mainly derived from xanthine oxidase (XO), and that reversal of increased ROS formation corrects its function and improves Ca^{2+} handling.

EXPERIMENTAL PROCEDURES

We studied male spontaneous hypertensive-heart failure rats SHHF (~18 months old) and their normotensive controls, Wistar-Kyoto rats as previously described (12). Heart failure was confirmed using echocardiography (see the supplemental material). The Animal Care and Use Committee of the Miller School of Medicine of the University of Miami approved all protocols and experimental procedures.

Myocytes were isolated as described in detail in the supplemental material. Intracellular calcium was measured as previously described (5). Cell contractility was estimated measuring sarcomere length as previously described (5). The degree of sarcomere shortening is expressed as the ratio between the amplitude of the shortening (ΔL) and the base-line sarcomere length (L_0).

Assessment of SR Ca^{2+} Leak—Calcium leak was assessed as described by Shannon *et al.* (13, 14). Ventricular myocytes were loaded with fura-2 and paced by field stimulation at the different frequencies in normal Tyrode's solution until cellular Ca^{2+} transients reached a steady state. After the last pulse, the bath solution was rapidly switched to 0 Na^+-0 Ca^{2+} (Na^+ replaced by Li^+) Tyrode. In the control condi-

* This work was supported, in whole or in part, by National Institutes of Health Grants RO1HL 65455 and HL094849-01.

[S] The on-line version of this article (available at http://www.jbc.org) contains supplemental text and Figs. S1 and S2.

[1] Both authors contributed equally to this work.

[2] To whom correspondence should be addressed: Biomedical Research Bldg., 1501 N.W. 10th Ave., Rm. 824, P.O Box 016960 (R125), Miami, FL 33101. Tel.: 305-243-1999; Fax: 305-243-3906; E-mail: jhare@med.miami.edu.

[3] The abbreviations used are: HF, heart failure; RyR, ryanodine receptor; SR, sarcoplasmic reticulum; SHHF, spontaneously hypertensive heart failure; WKY, Wistar-Kyoto; XO, xanthine oxidase; NOS, nitric-oxide synthase; ROS, reactive oxygen species; DHE, dihydroethidium; TRITC, tetramethylrhodamine isothiocyanate.

tion, $[Ca^{2+}]_i$ was monitored, whereas 0 Na^+-0 Ca^{2+} Tyrode buffer was applied for 40 s to eliminate transsarcolemmal Ca^{2+} fluxes, creating a closed system with a steady state $[Ca^{2+}]_i$. Then a rapid pulse of caffeine (10 mM) was added to cause SR Ca^{2+} release. After the cell recovers, it was stimulated again in the same conditions, but the 0 Na^+-0 Ca^{2+} Tyrode solution contained 1 mM tetracaine. Under this condition, RyR was blocked, and a shift (decrease) in the fura-2 signal (cytosolic $[Ca^{2+}]$) was observed. In this condition, the leak was blocked, and the difference in $[Ca^{2+}]_i$ between tetracaine and control condition corresponded to diastolic Ca^{2+} efflux. The amplitude of the caffeine-induced Ca^{2+} transient was used to estimate the total $[Ca^{2+}]_i$. The load-leak relationship was constructed by grouping cells with similar total SR $[Ca^{2+}]$.

Direct Measurement of Intra-SR $[Ca^{2+}]_i$—Isolated myocytes were incubated with 1 μM mag-fura-2 acetoxymethyl ester (Molecular Probes Inc., Eugene, OR) for 1 h at room temperature. Then the cells were washed at least three times in normal Tyrode solution, for washout of the indicator out of the cytosol. The cells were used within 2 h for the experiments. With this protocol, 60–80% of the cells consistently displayed downward twitch and caffeine-induced transients, indication that the fluorescence signal originates preferentially from the SR. A similar protocol to fura-2 was used, including tetracaine in 0 Na^+-0 Ca^{2+} solution and caffeine.

S-Nitrosylation—For determination of RyR2 nitrosylation, the hearts were treated as previously described (9), and the biotin switch technique was performed accordingly to Jaffrey *et al.* (15). To visualize *S*-nitrosylation in cardiac sections, we applied the biotin switch method with modifications (16, 17). Briefly, fresh hearts were embedded in O.C.T. (Tissue-Tek), frozen, cut in 10-μm sections, and fixed in microscope slides. The sections were washed in HEN buffer (see the supplemental material) and fixed with paraformaldehyde 2% for 20 min at room temperature and permeabilized with HEN plus Triton 1%. Sulfhydryl groups were blocked by incubating the slides with HEN-plus 20 mM *N*-ethylmalemaide for 30 min at 4 °C. After removal of permeabilizing and blocking solutions, the sections were incubated with 1 mM sodium acorbate and 3-[*N*-(maleimidopropionyl)] biocitin (MBP) as labeling agent, for 1 h at room temperature and then incubated with streptavidin-FITC at 4 °C. The nuclei were stained with DAPI. To visualize *S*-nitrosylation in isolated cardiomyocytes, we used a rabbit polyclonal anti-*S*-nitrosocysteine antibody (Sigma).

Detection of Superoxide—Fresh, unfixed hearts were frozen in O.C.T. (Tissue-Tek). Transverse sections (20 μm thick) were cut in a cryostat and placed on glass slides. The samples were then incubated at room temperature for 30 min with dihydroethidium (DHE, 3 μM; Molecular Probes). After washing with PBS, the sections were fixed with 2% paraformaldehyde for 5 min at 4 °C. Finally, the samples were mounted in Prolong Gold anti-fade (Invitrogen). The images were obtained using a Zeiss LSM-710 confocal microscope. Fluorescence was quantified using the Image-Pro plus software (MediaCybernetics, Silver Spring, MD).

Quantification of RyR2 Free Thiols—Free thiols in the RyR2 were assessed using the fluorescent probe for cysteines monobromobimane (Calbiochem, San Diego, CA) as described previously (5). Proteins were resolved in 3–8% Tris acetate gels and transilluminated with UV light. Total RyR2 was identified upon silver staining of the gel and confirmed by Western blotting with anti-RyR2. Free cysteine content is expressed as the ratio of the optical density of the UV signal to the total RyR signal.

Confocal Microscopy—Heart sections and isolated myocytes were prepared as described above, fixed in paraformaldehyde 2%, and incubated overnight at 4 °C with monoclonal antibodies to NOS1 (BD Bioscience), anti-RyR2 (Affinity BioReagent), and xanthine oxidase (NeoMarkers) and polyclonal antibodies against *S*-nitrosocysteine (Sigma), NOS1, and xanthine oxidase (Santa Cruz). Secondary incubations were performed at 37 °C for 1 h using anti-mouse TRITC and anti-rabbit FITC (Jackson Immunoresearch, West Grove PA) using a Zeiss LSM-710 confocal microscope. To validate the specificity of the signal obtained with the anti-*S*-nitrosocysteine antibody, we performed two controls: first, we used normal rabbit serum instead of the antibody, and second, before incubating with anti-*S*-nitrosocysteine antibody, the samples were treated with $HgCl_2$ (0.2% in PBS, 30 min) to degrade the *S*-nitrosylation bonds (18).

Co-localization Analysis—Quantitative co-localization analysis was performed after the images were deconvolved, using Huygens Essential software (Scientific Volume Imaging, Hilversum, The Netherlands) computing the Pearson correlation coefficient, as recommended (19, 20).

Statistical Analysis—The data are expressed as the means ± S.E. For comparisons of two groups, Student's *t* test was used. For comparison of three or more groups, one- or two-way analysis of variance was performed with Newman-Keuls post-hoc test. For both tests, a p value of less than 0.05 was considered significant.

RESULTS

Previously, we described increased XO activity in the SHHF rat heart (12). To confirm this, we measured an abundance of XO. Using immunofluorescence (Fig. 1*A*), we found that XO expression was increased in heart tissue sections of failing hearts compared with nonfailing (34.4 ± 5.6 fluorescence units in WKY *versus* 91.8 ± 11.2 in SHHF, $p < 0.005$). Up-regulation of XO was confirmed by Western blot analysis (Fig. 1*B*). Furthermore, at the single myocyte level at high magnification (Fig. 1*C*), it can be appreciated that the localization of XO is in close vicinity to the RyR2. In fact, the degree of co-localization between both proteins is increased in the failing hearts ($p < 0.0001$), consistent with an up-regulation of XO.

Redox State of RyR2—Given the proximity of XO and RyR2, it would be expected that an up-regulation of XO could alter the redox state of the channel, as well as its function. We previously described that decreased *S*-nitrosylation of the ryanodine receptor (RyR2) altered the channel activity, inducing sarcoplasmic reticulum Ca^{2+} leak and reducing

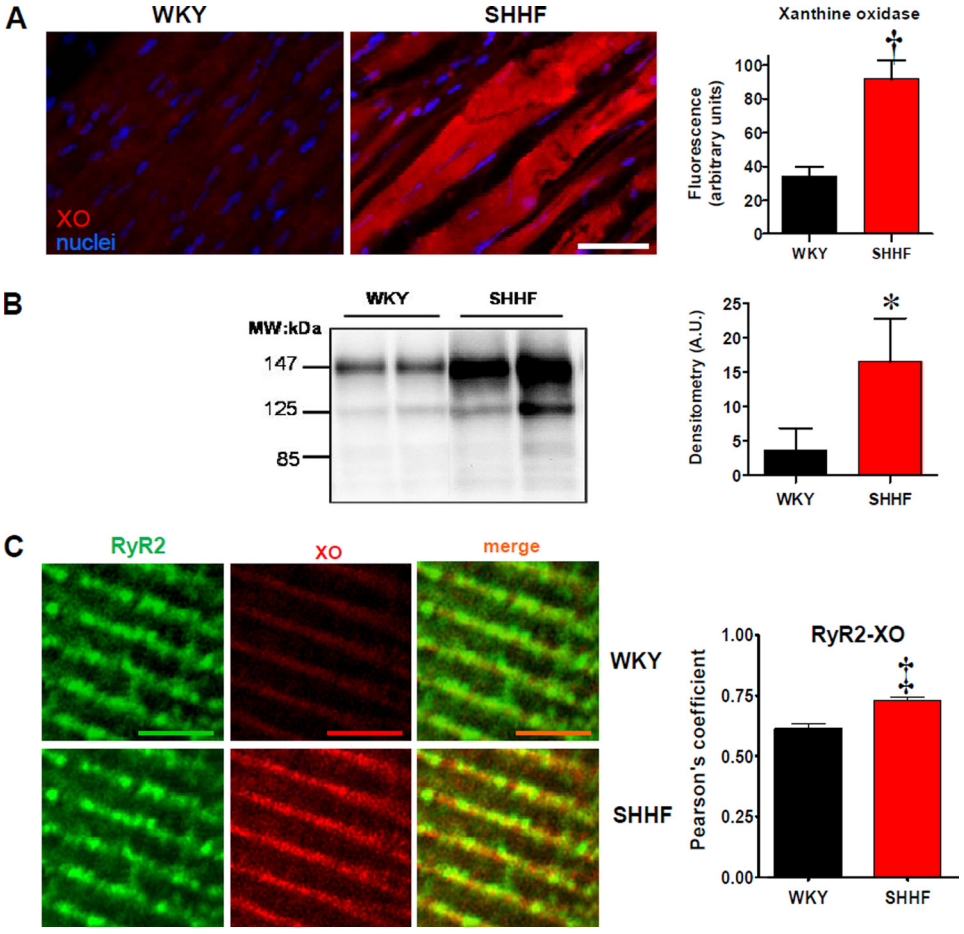

FIGURE 1. **Up-regulation of xanthine oxidase in heart failure.** *A*, immunostaining for XO in WKY and SHHF heart sections. The bar graph depicts average fluorescence signal ± S.E. of three hearts analyzed in each strain. The *bar* indicates 50 μm. *B*, Western blot analysis for XO expression in cardiac homogenates of WKY and SHHF hearts. The bar graph depicts average densitometry units ± S.E. $n = 4$ WKY hearts and 8 SHHF hearts. *MW*, molecular mass. *C*, double immunostaining for RyR2 (*green*) and XO (*red*) in isolated myocytes from nonfailing (WKY, $n = 15$ cells) and failing myocytes (SHHF, $n = 16$ cells). The *bars* indicate 100 μm. *Right panel*, bar graphs depicting the values for co-localization (Pearson coefficient values) analysis between both proteins. *, $p < 0.05$; †, $p < 0.005$; ‡, $p < 0.0001$.

contractility (5). We investigated here the degree of *S*-nitrosylation of RyR2 with the biotin switch assay (Fig. 2*A*). Consistent with the global histological studies, the level of *S*-nitrosylated RyR2 was lower in the failing hearts (5.6 ± 1.8 densitometric units in WKY *versus* 1.9 ± 1.0 in SHHF, $p < 0.05$, $n = 5$ WKY and 6 SHHF hearts). Next, we measured the levels of free thiols (SH-RyR2) using the monobromobimane assay (Fig. 2*B*). Relative free thiols levels were lower in the failing hearts (14.1 ± 1.4 densitometric units in WKY *versus* 9.5 ± 1.0 in SHHF, $p < 0.05$, $n = 3$ WKY and 4 SHHF hearts), suggesting, along with decreased *S*-nitrosylation, increased oxidation of cysteine residues. Finally, we analyzed the amount of phosphorylated RyR2 in serine 2809, because this modification has been related to RyR2 leak and the progression to HF (21). There were no differences in the ratio of phosphorylated to total RyR2 between strains, although both were intensively phosphorylated (0.89 ± 0.07 WKY, $n = 4$ *versus* 0.80 ± 0.06 SHHF, $n = 5$). Together, these results strongly suggest that in heart failure, RyR2 has lost *S*-nitrosylated cysteines, and they are highly oxidized.

A decrease in expression of NOS may have been the cause of decreased *S*-nitrosothiols. For this reason, we evaluated the level of the three NOS isoforms (Fig. 2*C*). NOS1 was increased (both α and μ isoforms), consistent with previous reports in heart failure (22, 23). NOS3 levels were not different between strains, and NOS2 expression was below our limit of detection. These results suggest that changes in NOS expression are not a cause for decreased *S*-nitrosylation in this model of heart failure.

Nitroso-redox Pathways—We studied the levels of nitrogen reactive species (*S*-nitrosylation) and ROS in WKY and SHHF hearts (Fig. 3). The levels of ROS detected by oxidative microphotography with DHE staining (Fig. 3*A*) were increased in the heart failure rats. Perfusion of isolated hearts with the xanthine oxidase inhibitor oxypurinol (100 μM, 45 min) decreased the levels of ROS in the failing hearts to levels similar to the nonfailing hearts.

S-Nitrosylation—Next, we assessed global myocardial *S*-nitrosylated proteins. We applied a modified biotin switch protocol for *in situ* detection of nitrosylated proteins in fresh myocardial sections (Fig. 3*B*). The *S*-nitrosylation signal was diminished in the failing hearts compared with WKY ($p < 0.05$). The treatment with oxypurinol restored the levels of *S*-nitrosylation in the failing hearts to normal levels and even increased *S*-nitrosylation in WKY hearts ($p < 0.05$).

RyR2 Nitrosylation—To test whether increased XO activity had a causal relationship with the levels of nitrosylation of RyR2, we analyzed the level of *S*-nitrosylation of cardiac RyR2 in isolated myocytes treated with or without oxypurinol. Using confocal microscopy, we compared the degree of co-localization for RyR2 and *S*-nitrosocysteine in isolated cardiomyocytes. In WKY, a clear co-localization between RyR2 and *S*-nitrosocysteine was observed (Fig. 4). On the contrary, the co-localization was significantly decreased in SHHF myocytes, due mainly to the general reduction in *S*-nitrosothiols. Incubation with oxypurinol (100 μM, 60 min (24)) significantly increased the general level of *S*-nitrosylation ($p < 0.05$) and, in particular, the degree of *S*-nitrosylation associated with the RyR2. Thus, XO inhibition restored the redox state of RyR2.

Intracellular Ca^{2+} Handling and Contractility—To gain insights into the mechanistic impact of RyR2 redox restoration,

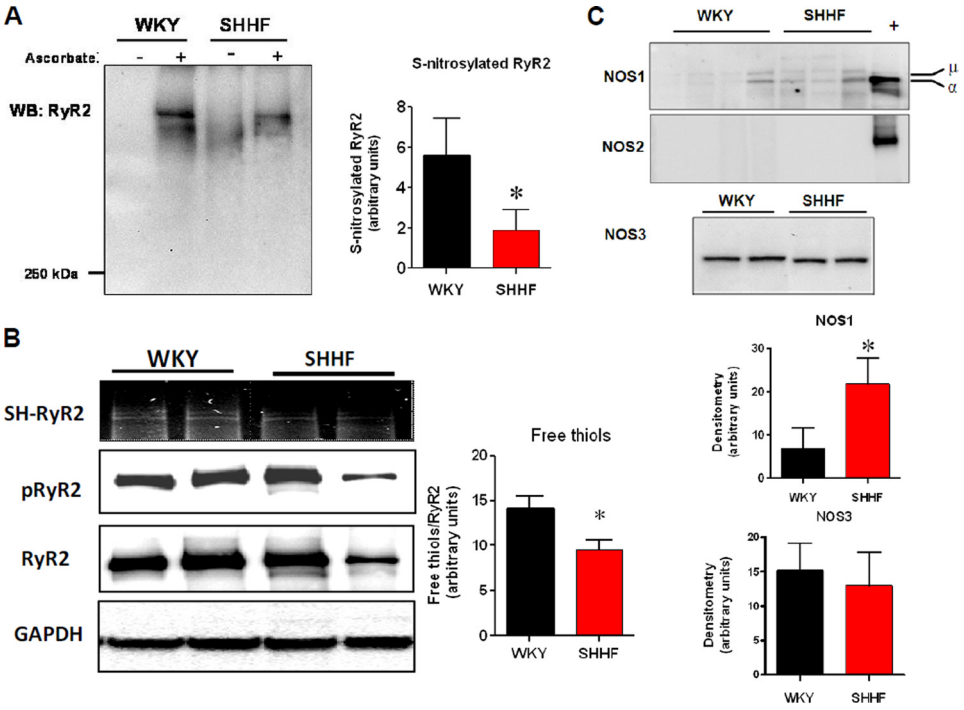

FIGURE 2. **Redox modifications of ryanodine receptor in heart failure.** *A*, biotin switch assay for *S*-nitrosylated RyR2 in nonfailing (WKY) and failing (SHHF) heart homogenates. Cardiac homogenates labeled for *S*-nitrosylation in the presence or absence of sodium ascorbate as the negative control of the assay. The bar graph depicts the average densitometry values ± S.E. of $n = 5$ WKY and 6 SHHF hearts. *WB*, Western blotting. *B*, relative free thiols (SH-RyR2), phosphorylated RyR2 at Ser^{2809} (pRyR2), and total content in RyR2 in heart homogenates of WKY and SHHF rats. GAPDH was used as loading control. *C*, NOS isoform expression. *Top panel*, Western blot analysis for NOS1. + indicates positive control (rat brain homogenate), α and μ are spliced variants for NOS1. The bar graph shows average densitometry values ± S.E., $n = 4$ WKY hearts and 9 SHHF hearts. *, $p < 0.05$. *Middle panel*, Western blot analysis to test the presence of NOS2 in WKY and SHHF rat hearts. + indicates NOS2 positive control (a lysate of activated macrophages). *Bottom panel*, NOS3 in heart homogenates of nonfailing (WKY) and failing (SHHF) hearts. The bar graphs show average densitometry values ± S.E., $n = 4$ WKY hearts and 9 SHHF hearts. *, $p < 0.05$.

we investigated some components of the excitation-contraction coupling process in which the activity of RyR2 is a key regulatory element. To this end, we assessed contractility and calcium handling in this model by measuring sarcomere shortening of isolated myocytes and the amplitude of the Ca^{2+} transients (Fig. 5). When myocytes were paced from 0.5 to 4 Hz of stimulation, the degree of sarcomere shortening was relatively flat in WKY myocytes. Conversely, in SHHF myocytes, the response was negative, *i.e.* the degree of sarcomere shortening decreased with the increased frequency of stimulation as has been previously described (25) (Fig. 5*A*). This decrease in contractility was correlated with the levels of intracellular calcium. In WKY, the amplitude of the transients increased with frequency, but in the failing myocytes it remained relatively constant (Fig. 5*B*). In the failing myocytes, both cell contractility and Ca^{2+} transients were improved when the cells were incubated with oxypurinol (100 μM for 40 min). Shorter incubation times did not produce an effect, and oxypurinol did not affect contractility or calcium transients in WKY cells (data not shown).

Because diastolic SR Ca^{2+} leakage through RyR2 is an important factor affecting Ca^{2+} handling and content in heart failure, we evaluated this leak. For this, we measured the diastolic SR Ca^{2+} efflux using tetracaine as an inhibitor of RyR2 (Fig. 6*A*) as has been previously described (13, 14). When comparing the amount of Ca^{2+} leak at matched Ca^{2+} contents (assessed by caffeine application), we found an increased diastolic SR efflux in the failing myocytes. This was reduced by oxypurinol treatment to the levels of the nonfailing myocytes. We also assessed intra-SR Ca^{2+} directly using the low affinity Ca^{2+} ($K_d = 50$ μM) indicator mag-fura2 (Fig. 6*B*). Using mag-fura2, the Ca^{2+} transient is shown as a downward shift, because it denotes the Ca^{2+} content within the SR. Upon caffeine application, SR is emptied of Ca^{2+}. Using this technique, we found that the intra-SR Ca^{2+} content is significantly reduced in failing myocytes. Incubation of myocytes with oxypurinol (100 μM, 40 min) restored the SR Ca^{2+} content toward the value observed in the nonfailing myocytes. Together, these results demonstrate that the redox imbalance created by XO up-regulation directly impacts on the calcium-cycling process, particularly at the level of the RyR2, because of its high redox dependence.

DISCUSSION

In the present study, we show the consequences of the imbalance between reactive nitrogen and reactive oxygen species on excitation-contraction coupling in heart failure (Fig. 7). We show that in HF the RyR2 has diminished levels of *S*-nitrosylation, associated with impaired calcium handling and contractility. These data demonstrate that a spectrum of thiol modifications can lead to excess activation of the RyR2 and subsequent leak of calcium in disorders of muscle contraction.

Our findings are in agreement with a substantial body of literature demonstrating thiol modification, either via *S*-nitrosylation or by oxidative modification, promoting alterations in protein function (see for reviews Refs. 26 and 27). In the case of the RyR1 and RyR2, *S*-nitrosylation increases the activity of the channel (8, 28–33). Physiologically, this enhances the function of the channel and thus excitation-contraction coupling. Disruption of this important mechanism can result from either hypernitrosylation or oxidation. We anticipate that the difference is due to nitroso-redox disequilibrium arising at least in part from the increase in the superoxide producing enzyme XO. In this case we confirm the up-regulation of xanthine oxidase, as previously reported (12), and its close localization to RyR2.

To the best of our knowledge, this is the first report of the levels of nitrosylation in a model of heart failure. It has been reported that RyR2 contains 89 cysteines, of which 21 are in

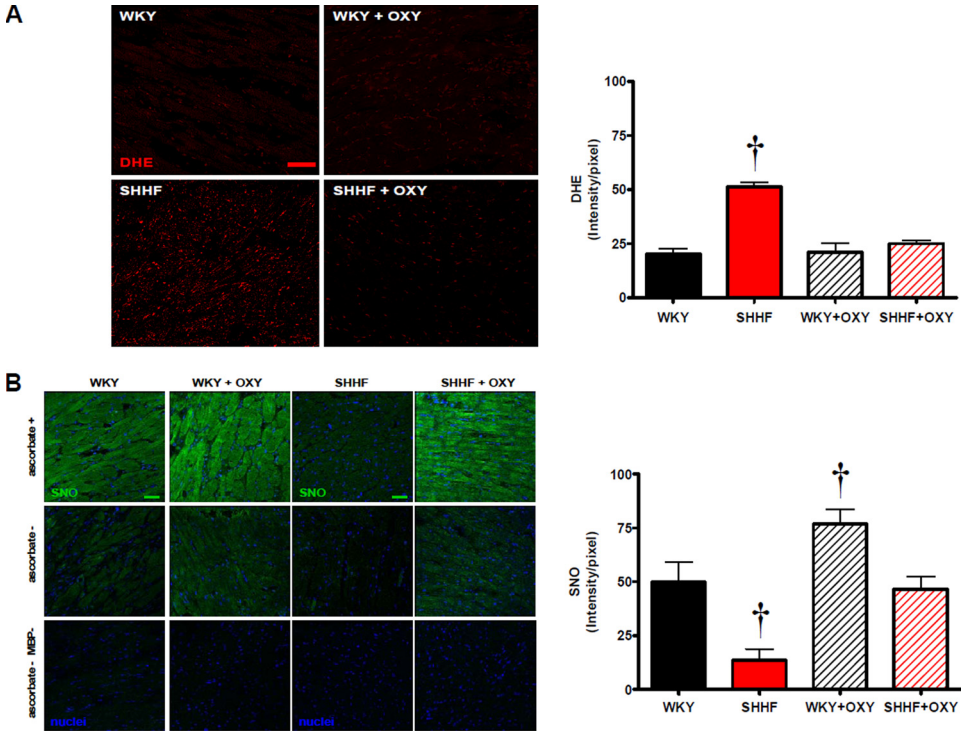

FIGURE 3. **Nitroso-redox imbalance in heart failure is restored by XO inhibition.** *A*, superoxide production assessed by DHE staining. Confocal images for the superoxide probe DHE of sections from WKY hearts, WKY hearts treated with oxypurinol (*OXY*, 100 μM, 45 min), SHHF hearts, and SHHF hearts treated with oxypurinol. The *right panel* indicates the quantification of the intensity for DHE, $n = 3$ hearts in each group; † indicates $p < 0.05$ *versus* all the other groups. *B*, set of panels of confocal microscopy signal for *S*-nitrosylation (*SNO*) sections of the same hearts as in Fig. 3*A*. Hearts of WKY rats (*upper set* of panels) and SHHF rats (*lower set* of panels) treated or not with oxypurinol (100 μM, 45 min) are shown. A modification of the biotin switch method was used. Labeling omitting ascorbate (*ascorbate −*) and ascorbate and the labeling agent MBP (*ascorbate − MBP −*) are presented as controls. The *bars* indicate 100 μm. *Right panel*, graph depicting average fluorescence signal ± S.E., $n = 3$ in each group. †, $p < 0.05$ *versus* all the other groups.

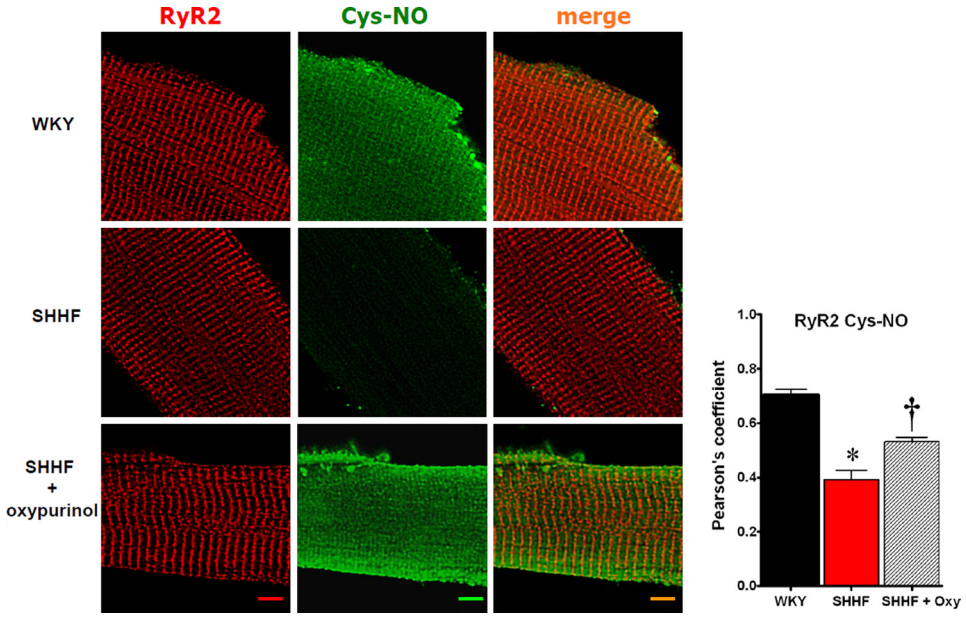

FIGURE 4. ***In situ* analysis of ryanodine receptor *S*-nitrosylation and impact of XO inhibition.** Confocal microscopy images of single cardiac myocytes immunostained for RyR2 (*red*) and *S*-nitrosocysteine (*Cys-NO*, *green*). The images were deconvolved, and the degree of co-localization was analyzed. WKY (nonfailing myocytes), SHHF (failing myocytes nontreated), and SHHF + oxypurinol (failing myocytes treated with oxypurinol 100 μM, for 60 min). The *upper bar graph* depicts the values for the Pearson coefficient of correlation for co-localization, $n = 13$ cells WKY, 23 SHHF, and 15 SHHF + oxypurinol). The *lower panel* indicates the intensity for *S*-nitrosocysteine signal. The *bars* indicate 10 μm. *, $p < 0.001$ *versus* WKY and SHHF + oxypurinol, $n = 19$ cells WKY, 40 SHHF and 36 SHHF + oxypurinol. †, $p < 0.01$ *versus* WKY and SHHF untreated.

the free (fully reduced) form (8). Thus, 68 cysteines may exist as *S*-nitrosylated, as *S*-glutathionylated, or as disulfide bonds. Our current data suggest that a significant portion of these *S*-nitrosylated residues are further oxidized in the failing heart. We show increased Ca^{2+} leak in a model of heart failure, associated with decreased *S*-nitrosylation of the channel. We correlated this modification with functional parameters known to be affected by redox modifications, notably the activity of RyR2. Consistent with our observations, it has been described that in a canine model of heart failure, oxidation of RyR2 produces diastolic Ca^{2+} leak in a manner that is partially reversed by reducing agents (34).

The origin of altered RyR2 activity apparently comes from nitroso-redox disequilibrium at the subcellular level (sarcoplasmic reticulum). Increased production of ROS derived from xanthine oxidase is likely to induce these redox modifications. Other mechanisms may include the general redox state of the cell, characterized by decreased GSH/GSSG ratio as we and others observed in models of HF (12, 34). Reduced *S*-nitrosylation and lower levels of free thiols are indicative of further oxidative modifications in cysteines. Consistent with our observations, it has been recently reported that *S*-nitrosoglutathione (35) but not NO is the nitrosylating species for RyR2. This means that NO is necessary (as source) but not sufficient to cause RyR2 nitrosylation. In addition, *S*-nitrosothiols (endogenous and exogenous) have been shown to be cardioprotective in animal models of myocardial infarction (36) and ischemia-reperfusion (37–39).

Chemically, cysteine residues are susceptible to a spectrum of oxidative modifications that include oxidation to sulfenic (-SOH), sulfinic ($-SO_2^-$), and sulfonic acids ($-SO_3^-$) as well as disulfide bonds (-SS-) (6, 26). In the

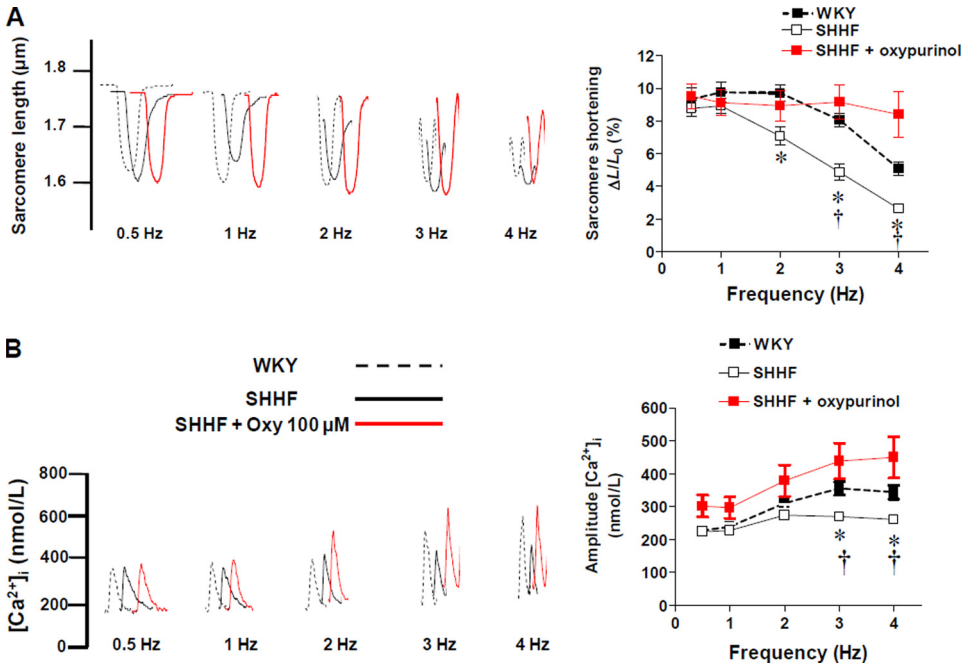

FIGURE 5. **Impaired contractility in heart failure is restored by XO inhibition.** *A*, representative traces of sarcomere shortening in nonfailing myocytes (WKY), failing myocytes (SHHF), and SHHF myocytes treated with oxypurinol 100 μM, paced at 0.5–4 Hz. *Right panel*, graph depicting average ± S.E. degree of sarcomere shortening ($\Delta L/L_0$), $n = 30$ cells/treatment. *B*, representative traces of calcium transients. *Right panel*, graph depicting average ± S.E. values for the amplitude of the calcium transients in WKY, SHHF, and SHHF myocytes treated with oxypurinol. $n = 10$–18 cells/treatment. *, $p < 0.05$ *versus* WKY; †, $p < 0.05$ *versus* SHHF + oxypurinol.

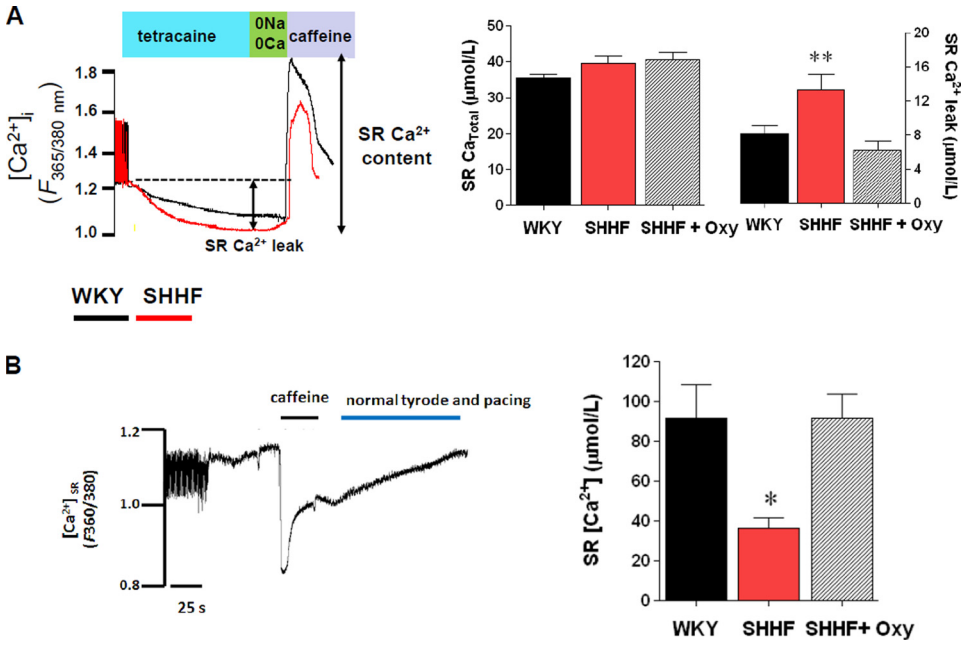

FIGURE 6. **Diastolic SR Ca^{2+} leak is reversed by XO inhibition.** *A*, protocol for assessment of SR Ca^{2+} leak. The cells are paced until a steady $[Ca^{2+}]_i$ is observed, then the pacing is stopped, and the bathing solution is changed to a 0 Na^+-0 Ca^{2+} solution containing tetracaine (1 mM), for 40 s. After this period, the solution is changed for ~5 s to a 0 Na^+-0 Ca^{2+} solution without tetracaine, and then a pulse of caffeine (10 mM) is applied to release the Ca^{2+} of the SR. The shift in the Ca^{2+} during tetracaine application accounts for the diastolic Ca^{2+} efflux from the SR. The bar graphs indicate comparison of SR leak (*left bar graph*) at a matched Ca^{2+} load for the three groups (*right bar graph*). *, $p < 0.05$ *versus* WKY and SHHF + oxypurinol (*Oxy*), one-way analysis of variance. *B*, direct assessment of SR Ca^{2+} content using mag-fura. *Left panel*, representative trace of sarcoplasmic reticulum $[Ca^{2+}]$. The cells were paced in normal solution; then tetracaine is applied to obtain an F_{max} for SR $[Ca^{2+}]$. Then the solution is changed for 0 Na^+-0 Ca^{2+}, to wash tetracaine without disturbing SR Ca^{2+} content, and caffeine is applied to release Ca^{2+} from the SR and obtain a F_{min} value. *Right panel*, average ± S.E. for SR Ca^{2+} content in nonfailing myocytes (WKY), failing nontreated myocytes (SHHF), and failing myocytes treated with oxypurinol 100 μM, 60 min. *, $p < 0.05$ *versus* WKY and SHHF + oxypurinol.

case of RyR, disulfide bonds have been described (40). Other forms of oxidation of the channel have not been explored to the best of our knowledge.

Another potential consequence of nitroso-redox imbalance could arise from xanthine oxidase-induced denitrosylation, both by superoxide-dependent or -independent ways. It has been shown that xanthine oxidase activity can decompose *S*-nitrosoglutathione and *S*-nitrosocysteine (41–43). As discussed above, only *S*-nitrosoglutathione is able to nitrosylate RyR2.

Hyperphosphorylation of RyR2 is another proposed mechanism for increased SR leak in HF. Phosphorylation of RyR2 at serine 2809 (21) and serine 2815 (44, 45) has been associated with increased RyR2 activity. We measured serine 2809 and found no difference in the degree of phosphorylation, but we did not measure serine 2815. We cannot exclude the possibility that this phosphorylation contributes to SR Ca^{2+} leak in the SHHF model.

Our findings should be also viewed in the context of descriptions of RyR1 hypernitrosylation as a cause of SR leak in skeletal muscle. In murine models of skeletal muscle disease like central core disease, fatigue, and muscular dystrophy (2–4), hypernitrosylation of RyR1 has been linked to abnormal increases in channel activity. Indeed, an increased *S*-nitrosylation of RyR1 and RyR2 will be associated with increased activity, according to evidence obtained at the single channel level. These findings can be reconciled by the fact that nitrosative *versus* oxidative modifications can act on the same cysteines. In the case of heart failure, apparently oxidative stress prevails over the nitrosative stress observed in skeletal muscle pathologies. In skeletal muscle, NOS1 is located in the sarcolemma, whereas in the cardiac myocyte it is located in the SR, close to the channel, supporting

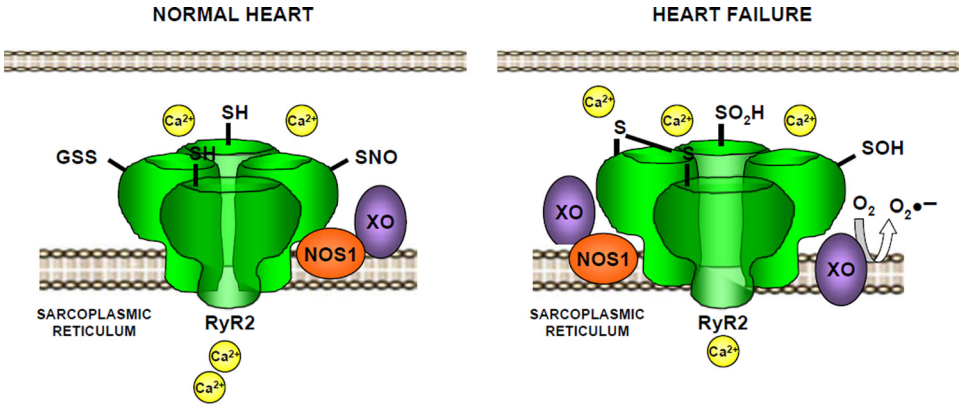

FIGURE 7. **Proposed working model for the effects of the XO-derived superoxide on RyR2 redox state and activity.** Under normal conditions, the redox state of the cardiac ryanodine receptor (RyR2) includes *S*-nitrosylation of cysteines, and the activity of the channel is normal. In heart failure, the excess of superoxide derived from XO impairs the normal nitrosylation of cysteines, which become oxidized (-S=S, -SOH, -SO_2H). In this condition, the activity of RyR2 increases, leading to diastolic leak that reduces the Ca^{2+} content of the sarcoplasmic reticulum.

physiologic RyR2 nitrosylation. Indeed, excess *S*-nitrosylation above normal levels will induce increased channel open probability in both RyR1 and RyR2. RyR1 in normal conditions contains approximately seven times more nitrosylated cysteines than RyR2 (8, 30). Increasing the degree of *S*-nitrosylated cysteines in RyR1 (nitrosative stress) as reported in disease states will dramatically increase the channel activity (leak). On the other hand, loss of normally *S*-nitrosylated cysteines in RyR2 caused by cysteine oxidation (oxidative stress) will also disturb RyR2 homeostasis leading to Ca^{2+} leak (34). This implies that a change in the normal content of *S*-nitrosylated cysteines in RyR in skeletal muscle and heart will have a detrimental impact in Ca^{2+} handling in both organs. Additionally, it has been recently described that reduced *S*-nitrosylation decreased the activity of RyR2 (46). Interestingly, this has been associated with the generation of a smaller amplitude of calcium transients (46). In other words, whatever the mechanism, the loss of RyR2 *S*-nitrosylation will have a profound impact on calcium handling, impairing cardiac contractility.

Although we focused on the effects of *S*-nitrosylation of the RyR2, it is evident from our results that other proteins as well as small molecules may be affected by the nitroso-redox imbalance observed in this model of heart failure. This may include other channels, proteins of the contractile apparatus, and elements of the mitochondria (37, 39), all of which are important regulators of excitation-contraction coupling and cardioprotection.

It has been previously described *in vitro* that xanthine oxidase-derived superoxide decomposes low molecular weight *S*-nitrosothiols such as *S*-nitrosoglutathione and *S*-nitrosocysteine. Given that *S*-nitrosoglutathione but not NO is the species that directly nitrosylates RyR2, we reasoned that any process that might interfere with *S*-nitrosoglutathione bioavailability would disrupt RyR2 nitrosylation. Indeed, our results show that neither NO levels nor NOS abundance are decreased in heart failure, but the nitrosothiol levels are clearly reduced. Importantly, we showed that nitrosothiol levels are restored by XO inhibition.

In conclusion, in the present study, we systematically and comprehensively document *S*-nitrosylation of RyR2 in failing myocardium. This decrease of *S*-nitrosylation is highly influenced by the production of ROS derived by the increased activity of XO. Inhibition of XO restores both the biochemical features of nitroso-redox imbalance and the calcium handling of cardiomyocytes toward normal. Together these findings demonstrate that hyponitrosylation of RyR2 directly impairs cellular Ca^{2+} handling. These findings offer important insights into the role NO/redox imbalance (47) plays in the failing myocyte and have therapeutic implications.

REFERENCES

1. Bers, D. M. (2006) *Physiology* **21,** 380–387
2. Bellinger, A. M., Reiken, S., Dura, M., Murphy, P. W., Deng, S. X., Landry, D. W., Nieman, D., Lehnart, S. E., Samaru, M., LaCampagne, A., and Marks, A. R. (2008) *Proc. Natl. Acad. Sci. U.S.A.* **105,** 2198–2202
3. Bellinger, A. M., Reiken, S., Carlson, C., Mongillo, M., Liu, X., Rothman, L., Matecki, S., Lacampagne, A., and Marks, A. R. (2009) *Nat. Med.* **15,** 325–330
4. Durham, W. J., Aracena-Parks, P., Long, C., Rossi, A. E., Goonasekera, S. A., Boncompagni, S., Galvan, D. L., Gilman, C. P., Baker, M. R., Shirokova, N., Protasi, F., Dirksen, R., and Hamilton, S. L. (2008) *Cell* **133,** 53–65
5. Gonzalez, D. R., Beigi, F., Treuer, A. V., and Hare, J. M. (2007) *Proc. Natl. Acad. Sci. U.S.A.* **104,** 20612–20617
6. Zimmet, J. M., and Hare, J. M. (2006) *Circulation* **114,** 1531–1544
7. Giordano, F. J. (2005) *J. Clin. Invest.* **115,** 500–508
8. Xu, L., Eu, J. P., Meissner, G., and Stamler, J. S. (1998) *Science* **279,** 234–237
9. Gonzalez, D. R., Fernandez, I. C., Ordenes, P. P., Treuer, A. V., Eller, G., and Boric, M. P. (2007) *Nitric Oxide* **18,** 157–167
10. Sánchez, G., Pedrozo, Z., Domenech, R. J., Hidalgo, C., and Donoso, P. (2005) *J. Mol. Cell Cardiol.* **39,** 982–991
11. Sánchez, G., Escobar, M., Pedrozo, Z., Macho, P., Domenech, R., Härtel, S., Hidalgo, C., and Donoso, P. (2008) *Cardiovasc. Res.* **77,** 380–386
12. Minhas, K. M., Saraiva, R. M., Schuleri, K. H., Lehrke, S., Zheng, M., Saliaris, A. P., Berry, C. E., Barouch, L. A., Vandegaer, K. M., Li, D., and Hare, J. M. (2006) *Circ. Res.* **98,** 271–279
13. Shannon, T. R., Ginsburg, K. S., and Bers, D. M. (2002) *Circ. Res.* **91,** 594–600
14. Shannon, T. R., Pogwizd, S. M., and Bers, D. M. (2003) *Circ. Res.* **93,** 592–594
15. Jaffrey, S. R., Erdjument-Bromage, H., Ferris, C. D., Tempst, P., and Snyder, S. H. (2001) *Nat. Cell Biol.* **3,** 193–197
16. Ckless, K., Reynaert, N. L., Taatjes, D. J., Lounsbury, K. M., van der Vliet, A., and Janssen-Heininger, Y. (2004) *Nitric Oxide* **11,** 216–227
17. Yang, Y., and Loscalzo, J. (2005) *Proc. Natl. Acad. Sci. U.S.A.* **102,** 117–122
18. Gow, A. J., Chen, Q., Hess, D. T., Day, B. J., Ischiropoulos, H., and Stamler, J. S. (2002) *J. Biol. Chem.* **277,** 9637–9640
19. Scriven, D. R., Lynch, R. M., and Moore, E. D. (2008) *Am. J. Physiol. Cell Physiol.* **294,** C1119–C1122
20. Zinchuk, V., Zinchuk, O., and Okada, T. (2007) *Acta Histochem. Cytochem.* **40,** 101–111
21. Wehrens, X. H., Lehnart, S. E., Reiken, S., Vest, J. A., Wronska, A., and

Marks, A. R. (2006) *Proc. Natl. Acad. Sci. U.S.A.* **103,** 511–518
22. Bendall, J. K., Damy, T., Ratajczak, P., Loyer, X., Monceau, V., Marty, I., Milliez, P., Robidel, E., Marotte, F., Samuel, J. L., and Heymes, C. (2004) *Circulation* **110,** 2368–2375
23. Damy, T., Ratajczak, P., Shah, A. M., Camors, E., Marty, I., Hasenfuss, G., Marotte, F., Samuel, J. L., and Heymes, C. (2004) *Lancet* **363,** 1365–1367
24. Kögler, H., Fraser, H., McCune, S., Altschuld, R., and Marbán, E. (2003) *Cardiovasc. Res.* **59,** 582–592
25. Janssen, P. M., Stull, L. B., Leppo, M. K., Altschuld, R. A., and Marbán, E. (2003) *Am. J. Physiol. Heart Circ. Physiol* **284,** H772–H778
26. Hess, D. T., Matsumoto, A., Kim, S. O., Marshall, H. E., and Stamler, J. S. (2005) *Nat. Rev. Mol. Cell Biol.* **6,** 150–166
27. Handy, D. E., and Loscalzo, J. (2006) *Arterioscler. Thromb. Vasc. Biol.* **26,** 1207–1214
28. Aracena, P., Sánchez, G., Donoso, P., Hamilton, S. L., and Hidalgo, C. (2003) *J. Biol. Chem.* **278,** 42927–42935
29. Donoso, P., Aracena, P., and Hidalgo, C. (2000) *Biophys. J.* **79,** 279–286
30. Eu, J. P., Sun, J., Xu, L., Stamler, J. S., and Meissner, G. (2000) *Cell* **102,** 499–509
31. Hidalgo, C., Aracena, P., Sanchez, G., and Donoso, P. (2002) *Biol. Res.* **35,** 183–193
32. Marengo, J. J., Hidalgo, C., and Bull, R. (1998) *Biophys. J.* **74,** 1263–1277
33. Stoyanovsky, D., Murphy, T., Anno, P. R., Kim, Y. M., and Salama, G. (1997) *Cell Calcium* **21,** 19–29
34. Terentyev, D., Gyorke, I., Belevych, A. E., Terentyeva, R., Sridhar, A., Nishijima, Y., Carcache de, B. E., Khanna, S., Sen, C. K., Cardounel, A. J., Carnes, C. A., and Gyorke, S. (2008) *Circ. Res.* **103,** 1466–1472
35. Sun, J., Yamaguchi, N., Xu, L., Eu, J. P., Stamler, J. S., and Meissner, G. (2008) *Biochemistry* **47,** 13985–13990
36. Lima, B., Lam, G. K., Xie, L., Diesen, D. L., Villamizar, N., Nienaber, J., Messina, E., Bowles, D., Kontos, C. D., Hare, J. M., Stamler, J. S., and Rockman, H. A. (2009) *Proc. Natl. Acad. Sci. U.S.A.* **106,** 6297–6302
37. Lin, J., Steenbergen, C., Murphy, E., and Sun, J. (2009) *Circulation* **120,** 245–254
38. Sun, J., Picht, E., Ginsburg, K. S., Bers, D. M., Steenbergen, C., and Murphy, E. (2006) *Circ. Res.* **98,** 403–411
39. Sun, J., Morgan, M., Shen, R. F., Steenbergen, C., and Murphy, E. (2007) *Circ. Res.* **101,** 1155–1163
40. Aracena-Parks, P., Goonasekera, S. A., Gilman, C. P., Dirksen, R. T., Hidalgo, C., and Hamilton, S. L. (2006) *J. Biol. Chem.* **281,** 40354–40368
41. Aleryani, S., Milo, E., Rose, Y., and Kostka, P. (1998) *J. Biol. Chem.* **273,** 6041–6045
42. Jourd'heuil, D., Mai, C. T., Laroux, F. S., Wink, D. A., and Grisham, M. B. (1998) *Biochem. Biophys. Res. Commun.* **246,** 525–530
43. Trujillo, M., Alvarez, M. N., Peluffo, G., Freeman, B. A., and Radi, R. (1998) *J. Biol. Chem.* **273,** 7828–7834
44. Ai, X., Curran, J. W., Shannon, T. R., Bers, D. M., and Pogwizd, S. M. (2005) *Circ. Res.* **97,** 1314–1322
45. Guo, T., Zhang, T., Mestril, R., and Bers, D. M. (2006) *Circ. Res.* **99,** 398–406
46. Wang, H., Viatchenko-Karpinski, S., Sun, J., Gyorke, I., Benkusky, N. A., Kohr, M. J., Valdivia, H. H., Murphy, E., Gyorke, S., and Ziolo, M. (2010) *J. Physiol.* **588,** 2905–2917
47. Hare, J. M., and Stamler, J. S. (2005) *J. Clin. Invest.* **115,** 509–517